Catalysis Today 148 (2009) 130–133

Contents lists available at ScienceDirect

Catalysis Today

journal homepage: www.elsevier.com/locate/cattod

Combination of CO_2 reforming and partial oxidation of methane to produce syngas over Ni/SiO_2 prepared with nickel citrate precursor

Sufang He [a,b], Qiangshan Jing [c], Wanjin Yu [a], Liuye Mo [a,*], Hui Lou [a], Xiaoming Zheng [a]

[a] Institute of Catalysis, Zhejiang University, Key Lab of Applied Chemistry of Zhejiang Province, Hangzhou 310028, PR China
[b] Research Center for Analysis and Measurement, Kunming University of Science and Technology, Kunming 650093, PR China
[c] School of Chemistry and Chemical Engineering, Xinyang Normal University, Xinyang 464000, PR China

ARTICLE INFO

Article history:
Available online 14 April 2009

Keywords:
Methane
Syngas
CRPOM
Ni/SiO_2
Nickel citrate

ABSTRACT

The reaction of combination of CO_2 reforming and partial oxidation of methane to produce syngas (CRPOM) was tested over Ni/SiO_2 catalysts which were prepared via incipient-wetness impregnation using precursors of nickel citrate and nickel nitrate. The catalysts were characterized by X-ray powder diffraction analysis (XRD) and H_2-temperature-programmed reduction (H_2-TPR) techniques. It was shown that the nickel citrate precursor strengthened interaction between NiO and support to form nickel silicate like species which could be reduced to produce small crystallites of metallic nickel at high temperatures. The Ni/SiO_2 prepared with the nickel citrate precursor exhibited good catalytic performances for its highly dispersed metallic nickel derived from the nickel silicate species.

1. Introduction

The production of syngas from methane is one of the most promising utilization approaches of natural gas, which is now recognized to be one of the potential substitute resources for petroleum due to its abundant storage in the world. Nowadays, the significant technologies for the synthesis gas production from methane are based on endothermic reaction of carbon dioxide reforming (CDR) [1,2], exothermic reaction of partial oxidation of methane (POM) [3,4] and combination of these technologies (CRPOM). Compared to POM and CDR, CRPOM is a green and preponderant process: (1) energy coupling, (2) controllable product ratio of H_2/CO according to the need of the post-process, and (3) a safer operating environment.

The CRPOM was first studied in a fixed bed reactor by Vernon et al. [5]. However, from an engineering point of view, fluidized bed reactor was a good candidate for the CRPOM reaction [6], mainly for its symmetrical heat diffusion and less carbon deposition. For its good mechanical strength and high-surface area, spherical silica (SiO_2) is widely used as a catalyst support in fluidized bed reactor. In recent years, Ni-based catalysts have attracted considerable interest primarily due to their inexpensiveness and high activity compared to noble-metal-based catalysts. In our previous works [7,8], Ni/SiO_2 catalysts modified by MO_x (M: alkaline metal, alkaline earth metal, rare earth metal) prepared with nitrate precursor exhibited excellent resistance to carbon deposition and stable catalytic performance in fluidized bed reactor. However, a Ni/SiO_2 catalyst without addition promoter MO_x exhibited rapid deactivation after a short time reaction [7,8]. Recently, we found the Ni/SiO_2 catalysts prepared with the nickel citrate precursor were applied to the CRPOM reaction and showed a superior catalytic performance [9]. It was also reported that nickel citrate was a good precursor for preparation of highly dispersed Ni/(Al)MCM-41 catalysts [10,11]. Systematic studies over the Ni/SiO_2 prepared with different precursors were done using TPR and XRD techniques in this paper.

2. Experimental

2.1. Catalyst preparation

Ni/SiO_2 catalysts were prepared with incipient wetness impregnation. After impregnation, the samples were dried at 100 °C for 12 h and subsequently calcined in air at 700 °C for 4 h. The Ni/SiO_2 prepared with nickel nitrate and nickel citrate were designated as ANiSN and ANiSC (*A*% is weight percent of Ni on the catalysts), respectively.

The nickel citrate precursor was prepared as following procedure. An equal molar ratio of nickel carbonate and citric acid was mixed together. De-ionized water was added into the mixture, and then heated at ~100 °C until nickel carbonate was dissolved to form a green and transparent solution.

SiO_2 (S_{BET} = 498.8 m^2/g) is a commercial product provided by Nanjing Tianyi Inorganic Chemical Factory. SiO_2 was pretreated

* Corresponding author.
E-mail address: moliuye@zju.edu.cn (L. Mo).

0920-5861/$ – see front matter © 2009 Elsevier B.V. All rights reserved.
doi:10.1016/j.cattod.2009.03.009

with 5% HNO_3 aqueous solution for 48 h at room temperature and then fully washed with de-ionized water until the filtrate was neutrality. The size of SiO_2 was selected between 60 and 80 mesh.

2.2. Catalytic reaction

The catalytic reaction was performed in a fluidized-bed reactor that comprised of a quartz tube (I.D. = 20 mm, H = 750 mm) under atmospheric pressure at 700 °C. Prior to reaction, 2 mL of catalyst was reduced at 700 °C for 60 min under a flow of pure hydrogen at atmospheric pressure. A reactant gas stream that consisted of CH_4, CO_2, and O_2, with a molar ratio of 1/0.4/0.3, was used with a gas hourly space velocity (GHSV) of 9000 h^{-1}. The feed gases were controlled by mass flow controllers. The effluent gas cooled in an ice trap was analyzed with an online gas chromatograph equipped with a packed column (TDX-01) and a thermal conductivity detector. Under our reaction conditions, the oxygen in the feed gas was completely consumed in all cases. The conversions and the selectivities were calculated as the literature [7].

2.3. Catalyst characterization

2.3.1. X-ray powder diffraction analysis

X-ray powder diffraction (XRD) patterns of samples were obtained with an automated power X-ray diffractometer (Rigku-D/max-2550/PC, Japan) equipped with a computer for data acquisition and analysis, using Cu Kα radiation, at 40 kV and 300 mA. The reduced samples were prior reduced at 700 °C for 1 h and cooled to room temperature in hydrogen atmosphere, but the fresh samples were used directly after calcined in air at 700 °C for 4 h. The used catalysts were cooled from reaction temperature to room temperature under the atmosphere of Ar in the fluidized bed reactor. All the samples were ground to fine powder in an agate mortar before XRD measurements. The crystallite size of metallic nickel over supported nickel catalysts was estimated with the Scherrer equation.

2.3.2. H_2-temperature-programmed reduction

H_2-temperature-programmed reduction (H_2-TPR) experiments were performed in a fixed-bed reactor (I.D. = 4 mm). 50 mg sample was used and reduced under a stream of 5% H_2/N_2 (20 ml/min) from 50 °C to 800 °C at a ramp of 7 °C/min. Hydrogen consumption of the TPR was detected by a TCD and its signal was transmitted to a personal computer.

3. Results and discussion

3.1. Catalytic activity measurements

The catalytic activities of ANiSC and ANiSN are presented in Fig. 1. For the ANiSC catalysts, the conversion of CH_4 (X_{CH_4}) slightly increased from 72.9% to 76.7% with the loading of Ni from 1% to 3%. However, the X_{CH_4} of ANiSN showed drastically increase from 33.8% to 72.2% with the A from 1 to 5. The X_{CH_4} of ANiSC and ANiSN reached a plateau as A = 3 and 5, respectively. Evidently, the catalytic activity of ANiSC exhibited better than that of ANiSN, especially for the catalysts with low nickel loadings.

The effect of reaction temperature on the catalytic performance of 3NiSC was investigated (shown in Fig. 2). The conversions and selectivities increased with the reaction temperature. The X_{CH_4}, X_{CO_2}, S_{H_2} and S_{CO} increased from 45.7%, 13.1%, 79.0% and 76.0% to 95.5%, 95.9%, 98.7% and 99.7%, respectively, as the reaction temperature increased from 550 °C to 800 °C. High selectivity and conversion could be achieved at high reaction temperatures. This might be attributed to that low temperatures were inclined to

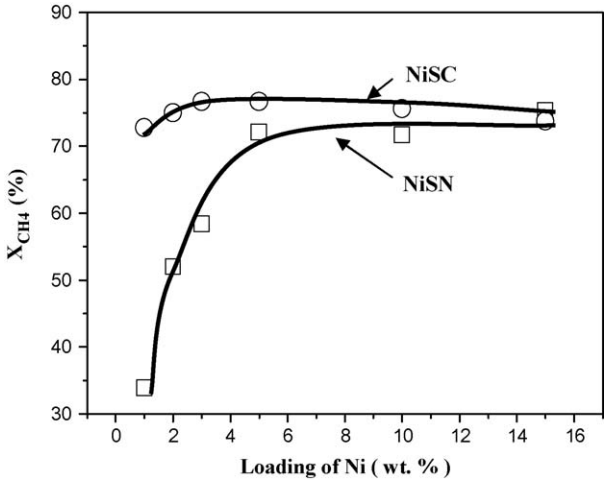

Fig. 1. Effect of different Ni loadings and precursors on catalytic activity.

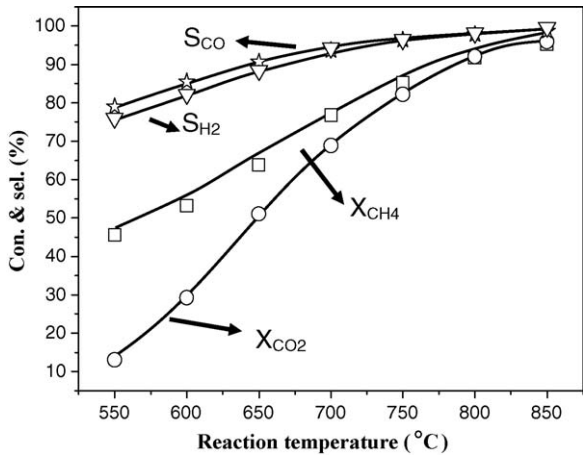

Fig. 2. Effect of reaction temperature on catalytic activity of 3NiSC.

complete combustion of methane, and high temperatures were prone to reforming and partial oxidation of methane [7].

The stabilities of 3NiSC and 3NiSN were also examined in Fig. 3. The catalysts prepared from nitrate precursors displayed a rapid decline of catalytic performance. The X_{CH_4} of 3NiSN was from 58.5% to 20.0% in 2 h reaction on stream. However, the NiSC showed a superior stability and the X_{CH_4} did not show any decline after 36 h reaction on stream. The deactivation of the 3NiSN was not caused

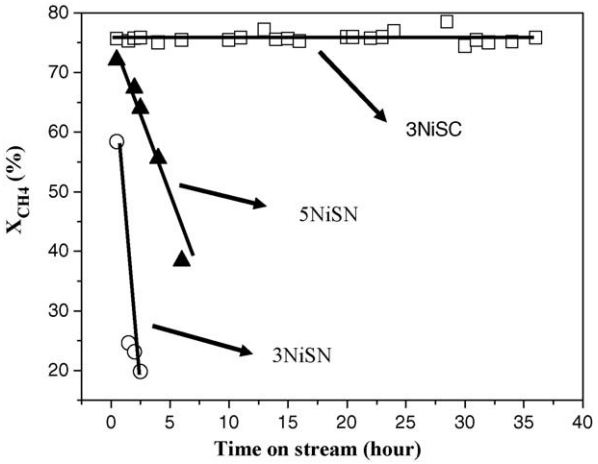

Fig. 3. Stability of 3NiSN, 5NiSN and 3NiSC catalysts.

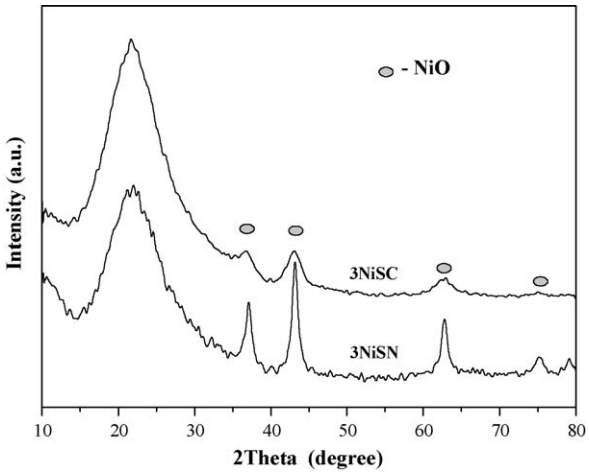

Fig. 4. XRD patterns of different catalysts calcined in air at 700 °C for 4 h.

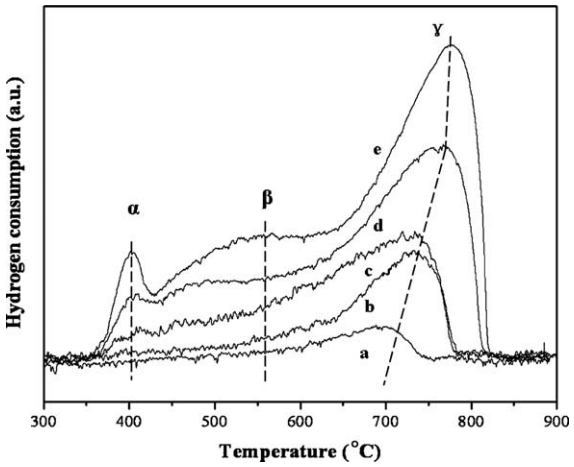

Fig. 6. The TPR profiles of the ANiSC catalysts calcined in air at 700 °C for 4 h (a: A = 1, b: A = 3, c: A = 5, d: A = 10, e: A = 15).

by carbon deposition but might be caused by sintering of nickel metal [8].

3.2. Catalyst characterization results

3.2.1. XRD study

The diffraction patterns for 3NiSC and 3NiSN catalysts are shown in Fig. 4. The NiO and amorphous SiO_2 phase was observed only. NiO diffraction peaks of the 3NiSC were broader than those of the 3NiSN, which indicated that the crystallite size of NiO over the 3NiSC was smaller than that of the 3NiSN.

The average crystallite sizes of metallic nickel over 3NiSC and 3NiSN catalysts, estimated by XRD and calculated using the Scherrer's equation, were presented in Fig. 5. The crystallite size of metallic nickel over the 3NiSN and 3NiSC was about 30.6 nm and 3.9 nm. The crystallite size of metallic nickel over the 3NiSC after 6 h reaction on stream was about 4.5 nm, which indicated that the 3NiSC showed excellent thermal stability. High dispersion of Ni over the 3NiSC might be a main reason for its excellent catalytic activity.

3.2.2. H_2-TPR results

Reduction behaviors of ANiSC catalysts ere exhibited in Fig. 6. The trails of TPR could be classified three groups: α, β and γ, which were located at ~400 °C, ~560 °C and >700 °C, respectively. The α and β peaks could be evidently observed as the A were >3 and >1, and the peak areas increased with the loading of nickel. The peak area of γ reasonably increased with the A. The temperature of γ peak shifted to high temperature from ~700 °C to ~770 °C as the A increased from 1 to 15. From above results, it could be deduced that the α peak might be the reduction of nickel oxide which showed negligible interaction with the support of SiO_2. The β peak could be ascribed to the reduction of nickel oxide which showed interaction with the support of SiO_2. The γ peak was also observed in literature [11] and was assigned to the reduction of the NiO species chemically bounded with Al-MCM-41. But in this paper, the γ peak might be originated from the reduction of nickel silicate like species [9]. The species over ANiSC catalysts detected by XRD were NiO and amorphous silica (shown in Fig. 4). Therefore, the assignment of γ peak to the reduction of nickel silicate like was reasonable. The species of nickel silicate like might be formed by a strong interaction between NiO and SiO_2. In order to elucidate the TPR results, a simplified model was shown in Fig. 7. The model exhibited that the nickel oxide which showed a weak interaction with the support of SiO_2 would be formed after the support was covered by a layer of nickel silicate like species.

The TPR profiles of the ANiSN are depicted in Fig. 8. It can be seen from Fig. 8 that there are great differences between the ANiSN and the ANiSC. The ANiSN were completely reduced at <550 °C. The reduction profiles could be divided into two groups: α peak and β peak. The α peak and the β peak located at <440 and ~460 °C. The temperature of α peak shifted from ~440 °C to ~410 °C as the A increased from 1 to 10, which indicated that the α peak might be contributed to the reduction of large crystallite of nickel oxide which

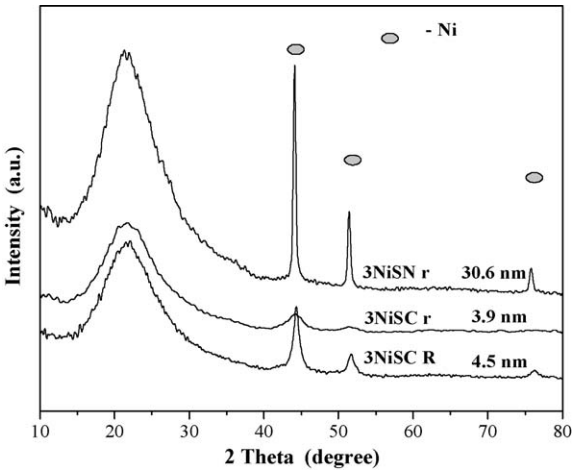

Fig. 5. XRD patterns of catalysts before and after reaction (R: the catalyst after reaction for 6 h; r: the catalysts after reduction by H_2 at 700 °C for 1 h).

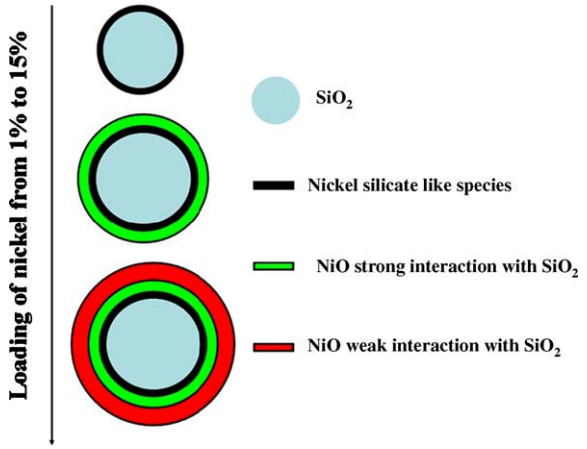

Fig. 7. Model of the nickel species distribution on the ANiSC catalysts.

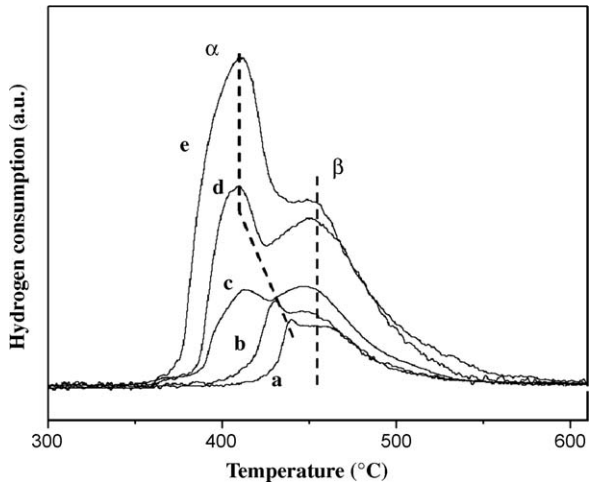

Fig. 8. TPR profiles of the ANiSN catalysts calcined in air at 700 °C for 4 h (a: A = 1, b: A = 3, c: A = 5, d: A = 10, e: A = 15).

is negligible weak interaction with SiO_2. The β peak was caused by the reduction of nickel oxide which interacted weakly with SiO_2 [9]. Noticeably, no γ peak was observed in the ANiSN, which meant that no nickel silicate like species was form on the ANiSN. Comprehensively considering XRD and H_2-TPR results above, it could be deduced that the nickel silicate like species originated from the NiO strong interaction with the support of SiO_2 could be reduced to small crystallite metallic nickel. High dispersion of Ni over SiO_2 might be a crucial reason for high activity of ANiSC.

4. Conclusions

The catalytic performance of Ni/SiO_2 was significantly depended on the precursors of nickel. The nickel nitrate precursor resulted in large size particles of nickel and poor catalytic activity, especially for low Ni-loading over Ni/SiO_2 catalysts. However, as the nickel citrate precursor was used, the superior catalytic activity and stability were obtained over Ni/SiO_2 catalysts. The strong interaction between NiO and SiO_2 formed nickel silicate like species over the NiSC, which was the main reason for high nickel dispersion and effectively prevention nickel particle from sintering at high reaction temperatures.

Acknowledgements

We thank the financial supports of National Natural Foundation of China (no. 2043030, 20703035), Department of Science & Technology of Zhejiang Province (2005E10016) and Program for New Century Excellent Talents in University of Henan Province (2006HANCET-20).

References

[1] A.T. Ashcroft, A.K. Cheetham, J.S. Foord, M.L.H. Green, C.P. Grey, A.J. Murrell, P.D.F. Vernon, Nature 344 (1990) 319.
[2] V.R. Choudhary, A.M. Rajput, B. Prabhakar, A.S. Mamman, Fuel 77 (1998) 1803.
[3] A.T. Ashcroft, A.K. Cheetham, M.L.H. Green, P.D.F. Vernon, Nature 352 (1991) 225.
[4] H.Y. Wang, E. Ruckenstein, Appl. Catal. A: Gen. 209 (2001) 207.
[5] P.D.F. Vernon, M.L.H. Green, A.K. Cheetham, A.T. Ashcroft, Catal. Today 13 (1992) 417.
[6] Y. Matsuo, Y. Yoshinaga, Y. Sekine, K. Tomishige, K. Fujimoto, Catal. Today 63 (2000) 439.
[7] L.Y. Mo, X.M. Zheng, Q.S. Jing, H. Lou, J.H. Fei, Energy Fuels 19 (2005) 49.
[8] Q.S. Jing, H. Lou, L.Y. Mo, J.H. Fei, X.M. Zheng, J. Mol. Catal. A: Chem. 212 (2004) 211.
[9] S.F. He, H.M. Wu, W.J. Yu, L.Y. Mo, H. Lou, X.M. Zheng, Int. J. Hydrogen Energy 2 (2009) 839.
[10] D.J. Lensveld, J. Gerbrand Mesu, A.J. van Dillen, K.P. de Jong, Microporous Mesoporous Mater. 44–45 (2001) 401.
[11] K. Fang, J. Ren, Y. Sun, J. Mol. Catal. A: Chem. 229 (2005) 51.